International Journal of Aviation Science and Technology

Research Article

Aerodynamic Investigation of Fixed - Pitch Aircraft Propeller

Erdogan Kaygan[1*], Dogukan Dogan[2], Ozan Mahir Alpagut[3]

[1] *Lentatek Space Aviation and Technology Inc., Ankara, Türkiye*
erdogan.kaygan@lentatek.com - 0000-0003-3319-3657

[2] *Lentatek Space Aviation and Technology Inc., Ankara, Türkiye*
dogukan.dogan@lentatek.com - 0009-0009-6993-0242

[3] *Lentatek Space Aviation and Technology Inc., Ankara, Türkiye*
mahir.alpagut@lentatek.com - 0009-0008-7913-0276

Abstract

An investigation of fixed - pitch propeller aerodynamics is described in this paper. The impetus for the work was to identify the proposed propeller's efficiency, thrust coefficient, power coefficient, and pressure contours. All computational analyses were performed using Computational Fluid Dynamics (CFD) software called Cradle scFLOW. During the simulation process, velocity was set to 60 knots (30.87 m/s) and the initial RPM (Revolution per Minute) was kept constant at 3100 to specify efficiency. Subsequently, the RPM value was varied to achieve thrust force. According to results, a thrust value of 1700N was achieved and propeller efficiency was found 0.79. Thrust value was then compared with the data obtained from experimental studies and the notable match was achieved. An increase in advance ratio was found to raise propeller efficiency at some point, and then reduction was observed in terms of efficiency due to thrust reduction. After these investigations, the obtained thrust force was compared with experimental data. The CFD results indicated a good agreement with the experimental results.

Keywords

Aerodynamics
CFD simulation
Propeller
Performance analysis
Propulsive efficiency

Time Scale of Article

Received 26 July 2024
Revised until 16 October 2024
Accepted 21 October 2024
Online date 27 November 2024

1. Introduction

A propeller is a device consisting of two or more blades that produces a flow of air towards the rear, which in turn provides the thrust to push an airplane forward. Thrust from a propeller is exerted along and parallel to the longitudinal axis of the device, and this axis coincides with the airplane's direction of motion. Propellers can be classified into two general types: fixed-pitch propellers and variable-pitch propellers. Most of the analysis necessary for understanding and designing both types is the same. Fixed-pitch propellers impart a fixed amount of thrust for a given power setting; that is, the total force exerted on the airplane is always the same for a given position of the throttle. The advantage of this configuration is its simple structure and cheap cost. However, the efficiency of FPP is slightly lower than that of a variable pitch propeller (VPP) due to the inconvenience of the appropriate pitch angle which is suitable for the aircraft state or flight condition. In contrast, a propeller pitch angle will be changed automatically in a variable-pitch propeller to accomplish any specific power. Most recent engine airplanes such as corporate and air transport aircraft use some type of variable-pitch propeller. However, in most modern general aviation airplanes (such as light training aircraft), fixed-pitch propellers are more affordable and less complex, and this is reason enough to consider their aerodynamic characteristics.

*: Corresponding Author Erdogan Kaygan, erdogan.kaygan@lentatek.com
DOI: 10.23890/IJAST.vm05is02.0203

Over the century, propellers have been an essential part of air transportation; unfortunately, these devices are far from remaining static technology. Though propellers have an extensive history, the recent era is marked by progressions in materials, computational capabilities, and aerodynamic perceptions. Combining all of these advancements is leading a revolution in propeller technology, enabling them to develop and meet the growing demands of industries endeavoring for enhanced performance, reduced environmental effect, and greater safety. The literature on propeller aerodynamics is scattered and, in some respects, inconsistent and incomplete. In this regard, summaries the theory of aircraft propellers by highlighting a systematic design procedures and deeper understanding of associated methods for computational performance models (Wald, 2006).

The propeller's design can alter any existing feature that the propeller's performance or adding a new feature on the propeller to improve its performance. For instance, increasing the number of blades positively impacts the blade's performance since the distribution of thrust and power is even in the propeller's wake. Therefore, the efficiency is slightly improved but not very significant. investigated the effects of blade numbers on aerodynamic performance of propellers (Bertetta *et al.*, 2012). Likewise, several researchers mentioned recent studies on different propeller design and analysis methods by using various experimental and computational methodologies (Ol et *al.*, 2008; Singh *et al.*, 2011; Asl *et al.*, 2017; Zao *et al.*, 2019). According to the results, it was observed that the rotation speed decreased as the number of blades increased. It has also been found to cause a decrease in propeller efficiency. However, increasing the number of blades will demand more power from the engine to produce thrust. For a given power and thrust, the propeller blades will be narrow as the number of blades increase. Having a large diameter propeller can significantly influence the performance, especially the propeller's efficiency. This is due to the ability to produce a greater fluid volume and better distribution of thrust and power compared to smaller diameter propeller. However, more power will be needed to rotate the propeller, can cause high fuel consumption and if it is an electric aircraft, the motor will potentially burn out.

Moreover, slotted propeller design concepts were also investigated by (Kutty *et al.*, 2017; Seeni *et al.*, 2019; Song *et al.*, 2019). (Ramzi *et al.*, 2011) investigated the performance variations of passive slotted blade in highly loaded compressor cascade. Slotted design on high cambered blade with

NACA 65-(18)10 airfoil sections were studied using CFD. The effect of slot location, slot width and slot slope on cascade performance was investigated. A reduction in pressure loss coefficient of up to 28.3% was observed among the various designs analyzed. Similarly, a numerical investigation of passive slotted wind turbine designed and investigated with S809 airfoil for Re of $2x10^6$(Kang and Park, 2013). Five different angles of attack cases were used. It was found that at 0.6 chord slot location and 14.24° angle of attack, the maximum lift coefficient (C_L) was observed. Furthermore, at 0.024chord and angles of attack of 14.24° and 20.15°, stall delay was observed. performed a slotted blade design study with slot opening extending from pressure side to suction side with slot width of 3 mm through both numerical and experimental methods (Xie *et al.*, 2013). The angles of attack are varied for identical flow conditions. It was found that at lower angle of attack from 0° to 10° the flow remained unchanged. At angle of attack of 20°, a 4.9% increase in C_L was observed. At 15° angle of attack, only a 1.6% increase in C_L value was found. Overall, taking CFD results into consideration, high rate of performance enhancement was achieved using slotted geometry. Additionally, better acoustic performance benefits were seen with higher number of blades (Lieser *et al.*, 1997).

Current conventional methodologies for predicting propeller performance are through momentum theory (McCormick, 1994) and blade element theory (Houghton and Carpenter, 2005). However, momentum theory is completely idealistic and completely independent of the airfoil to find performance parameters. Blade element theory, on the other hand, predicts performance relatively realistically by considering the airfoil as discrete wing elements. Nevertheless, both theories cannot reach the practical situation where the flow is truly complex due to the presence of 3D vortices created in the shear flow of the propeller. Using CFD enables to study viscous flow and to investigate the flow pattern across a propeller blade, which is not so applicable for other numerical methodologies (Kaidi, 2012). Comparing CFD simulation with experimental methods, CFD simulations was found to be less time required to obtain results. The numerical method in CFD is therefore chosen over other methods for the current study.

Ongoing research continues to uncover innovative design approaches, optimize performance through computational and experimental methods, and address the modern challenges of efficiency and environmental impact. In this paper, aerodynamic properties of proposed propeller model investigated by using CFD methods (application: Cradle scFLOW) and thrust data then validated through experimental data.

2. Method

Momentum and Blade element theory are the most common methods used to define aerodynamic

properties as aforementioned above in the introduction section. Due to complex flow regimes around the propeller geometry, both methods seem insufficient with an actual scenario. Hence, CFD has been used to identify the performance parameters a propeller blade.

2.1. CFD Governing Equations

In general, continuity and Reynolds-averaged momentum equations are the two main parts of the points while governing CFD equations (Versteeg et al., 1997). The continuity equation for an incompressible flow is given as follows:

$$\text{div } u=0 \tag{1}$$

Applying the Reynolds averaging approach (Osborne, 1845) to turbulence modeling produces time-averaged governing equations, also known as Reynolds Averaged Navier Stokes Equations (RANS) equations, which can be written in Cartesian tensor form as:

$$\frac{\partial \rho}{\partial t}+\frac{\partial}{\partial x_j}(\rho u_i)=0 \tag{2}$$

$$\frac{\partial(\rho\overline{u_l})}{\partial t}+\frac{\partial(\rho\overline{u_l u_j})}{\partial x_j}= -\frac{\partial \overline{p}}{\partial x_i}+\frac{\partial}{\partial x_j}\left[\mu\left(\frac{\partial \overline{u_l}}{\partial x_j}+\frac{\partial \overline{u_j}}{\partial x_i}-\frac{2}{3}\delta_{ij}\frac{\partial \overline{u_m}}{\partial x_m}\right)\right]+\frac{\partial}{\partial x_j}(-\rho\overline{u_l' u_j'}) \tag{3}$$

where x_i are Cartesian coordinates (i = 1,2,3); ρ is the density; t is the time; u_i are Cartesian velocity components (i = 1,2,3); $\overline{p}$ and μ indicate the pressure and dynamic viscosity, respectively, δ_{ij} represent the Kronecker delta, $-\rho\overline{u_l' u_j'}$ is the Reynolds stresses. Reynolds stresses can be related to mean deformation rates as indicated by the Boussinesq hypothesis (François, 2007) and can be written as:

$$-\rho\overline{u_l' u_j'} = \mu_t\left(\frac{\partial u_i}{\partial x_j}+\frac{\partial u_j}{\partial x_i}\right)-\frac{2}{3}\left(\rho k+\mu_t\frac{\partial u_i}{\partial x_i}\right)\delta_{ij} \tag{4}$$

where μ_t represents the turbulent viscosity. Then, μ_t will be estimated by the turbulence model equalities.

2.2 Propeller Model

The selected basic propeller was utilized with a diameter (D) of 1.45 m and a fixed pitch (β) of 11.5° (Fig. 1). The propeller is designed with estimated ARA-D 10% airfoil sections near the hub and Clark-Y airfoil sections near the tip. This propeller-like feature is commonly used in applications operating at low Reynolds number such as UAVs.

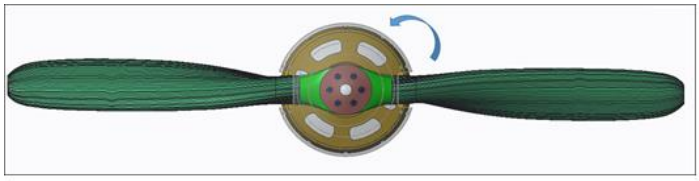

(a)

(b)

Fig. 1. Propeller model (a) Computer Aided Design model and (b) Structural model.

2.3 CFD Steady State-Rans Solver

In this study, the CFD finite volume-based solver Cradle scFLOW is chosen to solve the RANS equations for an incompressible flow. The flow around the propeller is always unstable, and the presence of turbulence patterns makes the flow unstable. However, the RANS turbulence model provides closure to the Reynolds Stress tensor, which signifies the influence of turbulent fluctuations in the mean flow. This allows steady-state simulations to be performed in Cradle scFLOW. The boundary conditions applied for this study are shown in Fig. 2.

2.4 Grid Generation and Flow Field Solution

3D numerical grid was applied in which the velocity components u, v and w and the pressure component p at the center of the control volumes are computed. The propeller was designed using Computer Aided Design software MSC Apex and then imported into Cradle SCFlow for domain creation. The simulation's flow domain is modeled based on the Multiple Reference Frame and consists of two regions: fixed and rotational (Fig. 2). A rotating reference frame that rotates at a constant angular speed of 3100 rpm surrounds the propeller. Subsequently, this value varied in order to measure how much thrust propeller can provide with diverse RPM settings.

The boundary conditions and computational domain are set according to (Seeni *et al.*, (2020) and (Sanjeevi *et al.*, 2009). The rotating reference frame is designed to have a cylinder-shaped geometry with a diameter of 1.1D. The fixed reference frame is assigned with a rectangular geometry with sides of dimensions 15Dx4Dx4D, as shown in Fig. 2. The adjusted dimensions were found to be sufficient for the simulation to reach steady state and for the trace of the flow to disappear below the impeller. An offset condition is set on rectangular walls while inlet and outlet labels are assigned to the front and back of the geometry. The carousel is maintained at a length of approximately 2D from the front of the geometry to 12D from the rear side of the geometry. The rotating frame is rotated at a small angle with the propeller set inside. The axis of rotation is adjusted to be aligned with the hub axis of the propeller.

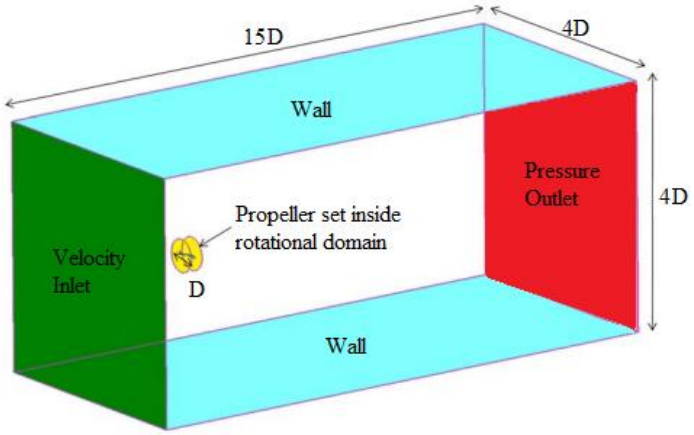

(a)

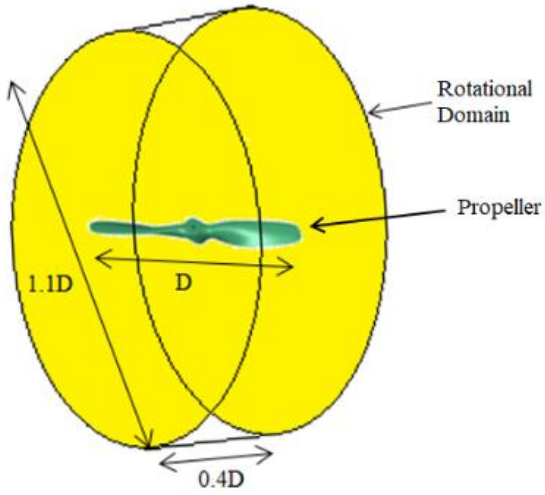

(b)

Fig. 2. Boundary conditions for (a) Stationary Computational Domain (b) Rotational-Computational Domain.

The area is connected using polyhedral elements in the two regions (Fig. 3). The mesh in the rotating frame close to the propeller is knitted with finer elements than the outer frame. Mesh generation is performed via simultaneous discretization in both regions using unstructured mesh. An unstructured mesh was chosen over structured network as both network schemes produced almost similar results. The curvature of the propeller geometry affected the mesh skew, which increased the complexity of the field geometry to be meshed. For an unstructured network, the number of Y+ walls to be protected in the fan wall must be less than 300 according to (Tian *et al.*, 2015) and (Alakashi *et al.*, 2014). The mesh independence study finds the right mesh resolution to get accurate results by reducing the simulation's errors. The accuracy of the result can be determined by comparing the results with existing experimental results.

The front and back parts of the fixed area are assigned as velocity input and pressure output, respectively. A no-slip condition is assigned to the wall of the rotating area. The turbulence intensity was set to 0.1% based on experimental assumptions (Brandt *et al.*, 2011). The output is specified with a static pressure of 0 Pa. The semi-indirect method for pressure linked equations is assumed as a pressure-velocity coupling diagram. It is assumed that the fluid is air at 20°C, with a density of 1.225 kg/m3 and a dynamic viscosity of 1.83x $kgm^{-1}s^{-1}$. Flow speed was set as 60 knots (30.87m/s).

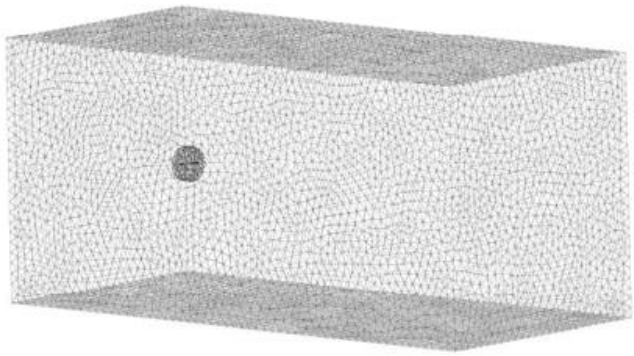

Fig. 3. Mesh-network structure created for propeller simulation.

2.5 Aerodynamic Coefficient and Propeller Efficiency

A relatively common and easiest method of computing the performance of a propeller is the use of Blade Element Theory. Using this method, the propeller split into many independent segments along its length. A balance of forces is applied to each section, including the thrust and torque generated by the segment and the lift and drag of the 2D section. At the same time, axial and angular momentum balance is applied. This yields a set of non-linear equations that can be solved iteratively for each blade section. The resulting cross-sectional thrust and torque values can be aggregated to estimate the overall performance of the propeller.

There are some performance parameters that need to be identified to shape out propeller characteristics aerodynamically. These parameters are:

- Thrust Coefficient (C_T): A dimensionless number that represents thrust performance relative to the air density, the propeller diameter, and the rotational speed.
- Power Coefficient (C_p): This dimensionless coefficient represents the power required to turn the propeller relative to the air density, diameter, and rotational speed.
- Efficiency (η): The ratio of the useful power (thrust power) generated by the propeller to the actual power input, expressed as a percentage.

The thrust coefficient is defined by the following expression:

$$C_T = \frac{T}{\rho n^2 D^4} \quad (5)$$

where T is the thrust force, ρ is the air density, n is the revolutions per second and D is the propeller's diameter. The advance ratio is defined by the following correlation:

$$J = \frac{V}{nD} \quad (6)$$

where V is the free stream velocity.

The power coefficient is defined as follows:

$$C_P = \frac{P}{\rho n^3 D^5} \quad (7)$$

The efficiency of the propeller is defined by the following correlation:

$$\eta = J\frac{C_T}{C_P} \quad (8)$$

Furthermore, propeller performance can be predicted by using the equation below;

$$\eta = \eta(C_P, J) \quad (9)$$

(Gur, 2013) proposed an example of such procedures. It should be noted that propeller power depends on torque and angular speed. Torque can be viewed as the resistive force due to rotation. Torque causes a twist from the hub towards the tip axis and is therefore undesirable.

2.6 Experimental Setup

The experimental studies were carried out by examining the propeller thrust generated on ground. The orientation and location of the accelerometer used during these tests are given in Fig. 4. The data were read from the Burster 8524-6020 type load cell placed on the engine test stand (relative linearity deviation: ±0.25%). The obtained data were later compared with the current numerical values.

3. Results and Discussion

3.1 Comparison between Numerical and Experimental Results of Thrust

Fig. 5 shows the comparison between CFD and experimental results. A maximum of 1700N were achieved with a maximum engine speed., Increasing propeller revolutions up to 3100 RPM tends to raise the thrust value further. This would be expected due to increased air component across the blades creating higher-pressure difference in order to accelerate aircraft, hence thrust increased. As can be seen from the graph (Fig. 5), experimental data are in close proximity with data obtained from Cradle scFLOW. There is a slight difference between the experimental and simulation results. This difference is observed because wind, speed and/or similar factors are not included in the simulation environment.

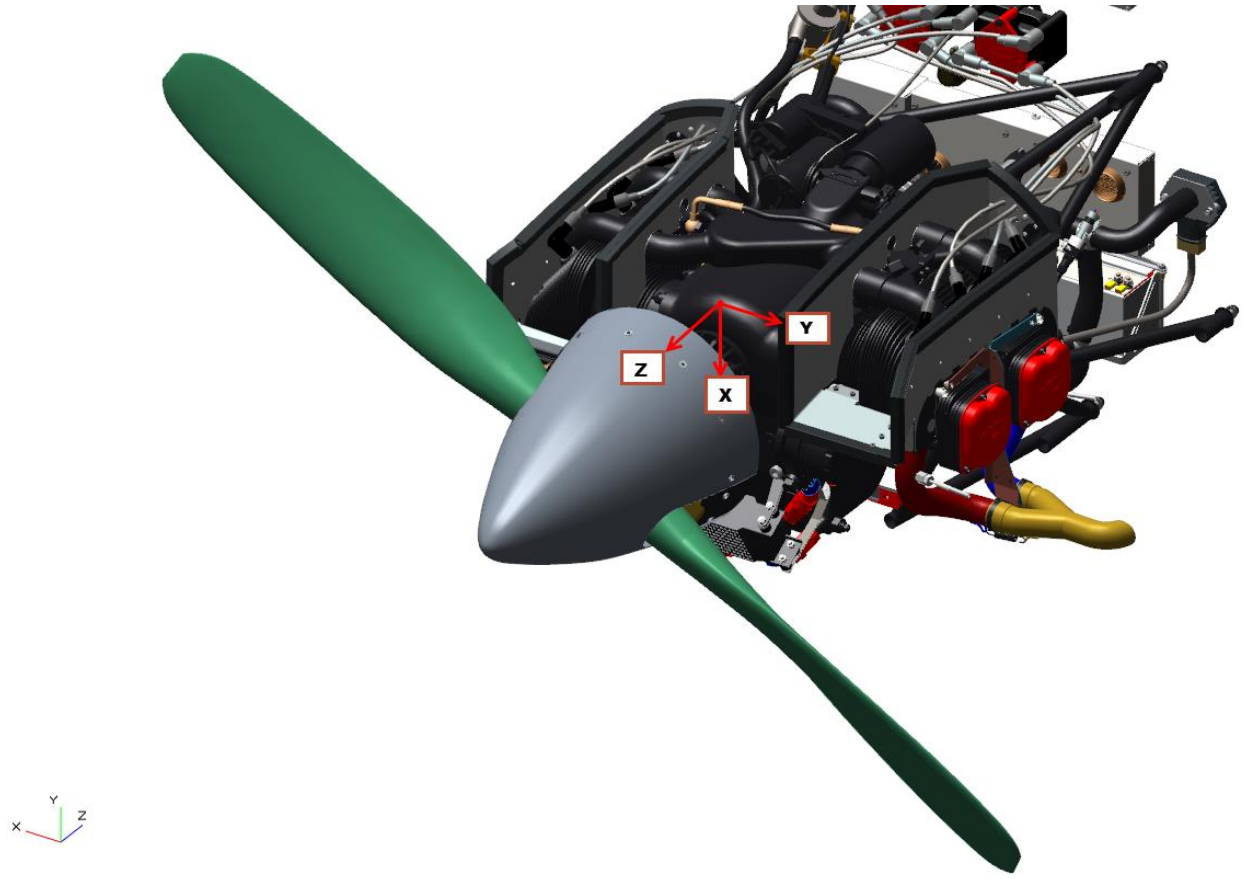

Fig. 4. Accelerometer attachment point and orientation of the coordinate system.

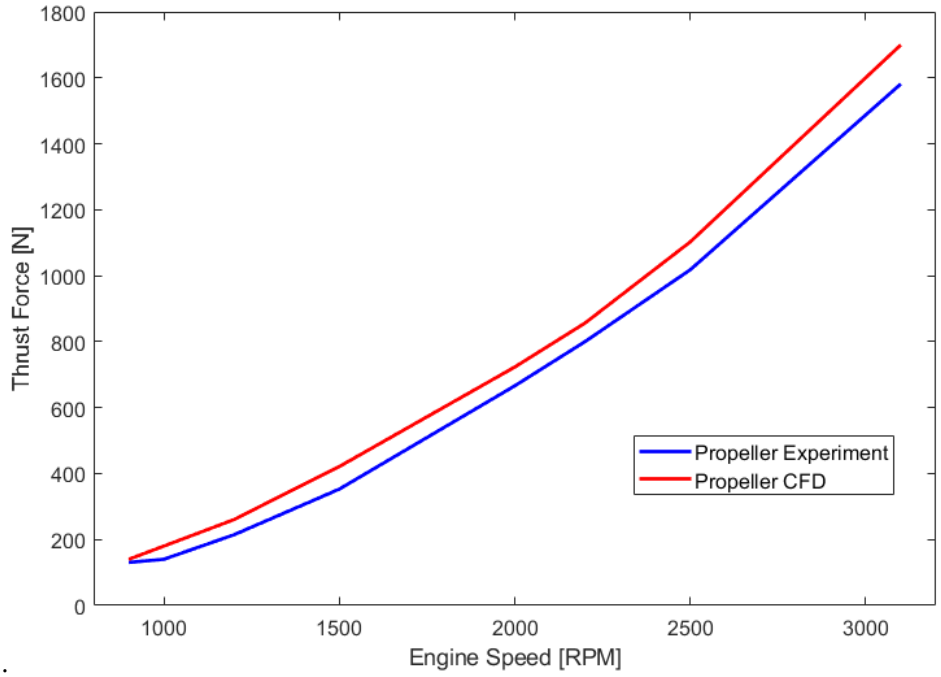

Fig. 5. Comparison between numerical and experimental results for thrust.

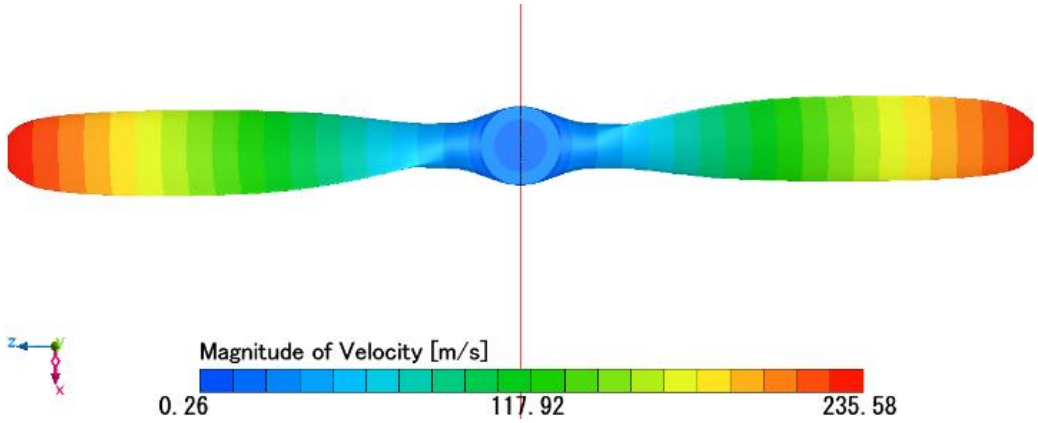

Fig. 6. Velocity distribution along the propeller.

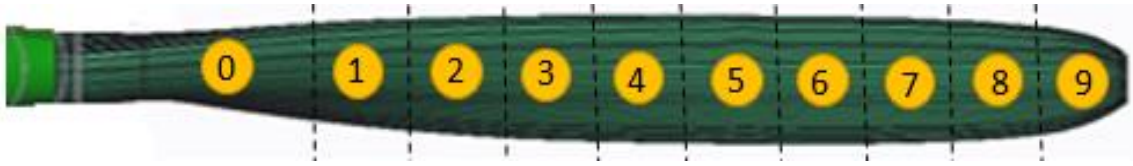

Fig. 7. Propeller sections.

3.2 Aerodynamic performance characterization of a propeller

It is a well-known concept that velocity distribution on the propeller varies according to the pressure distribution. It increases proportionally from the hub to the tip. Fig. 6 clearly shows the speed differences that gradually occur on the propeller. This distribution in speed values is evidence that the drag effect created by the propeller increases from the hub to the tip, as in theory (Marcus *et al.*, 2018). This would be expected, because when the rotating object is away from the center of rotation, the faster it moves.

In addition to the fixed pitch of the propeller, the amount of twisting also plays a role in shaping the fluidity and subsequently changing the values of the acting forces. The twist angle generally changes the angle of attack of the profile on the propeller, causing a decrease from the bottom of the blade to the tip, and then a non-linear lifting and drag force occurs (a decrease in force is expected at the tip point) as agreement with (Marcus *et al.*, 2018). The propeller sections are showing in Fig. 7. Fig. 8 (a) and (b) illustrate lift and drag forces obtained over the propeller surface. It can be seen that both drag and lift forces are increased up to some point around section 6 and then reduced as expected due to variation occurs at an angle of blades.

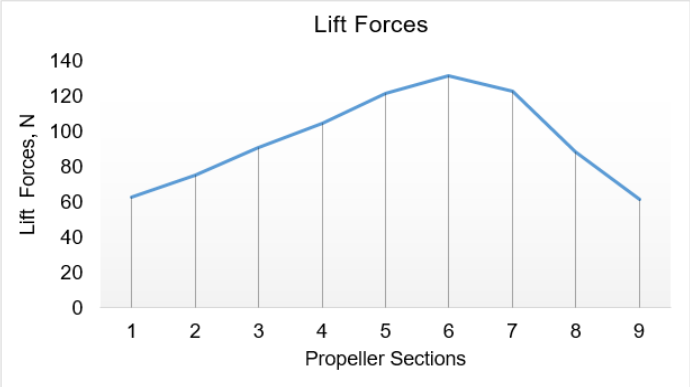

(a)

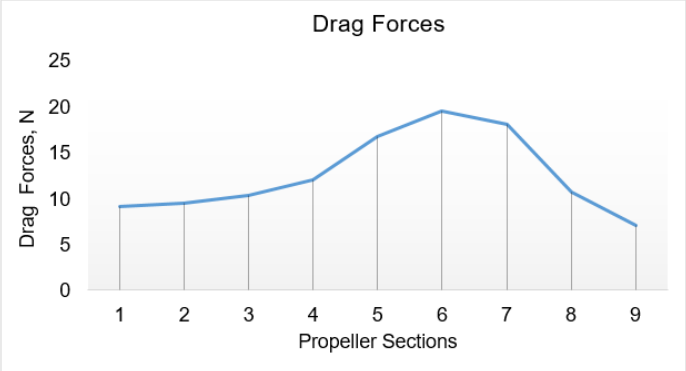

(b)

Fig. 8. Aerodynamic Forces produced by the propeller model (a) Lift and (b) Drag forces

Having the right distribution of lift and drag along the propeller blade often points out airfoils' composition in the blade. When the blade rotates, the propeller blade tip rotates faster than the blade section closer to the hub. Hence, the selection of airfoil along the blade is crucial due to this very reason.

Drag depends on several geometry properties including the airfoil shape, camber, thickness, etc., and on the operating conditions, Reynolds number, Mach number, and angle of attack. As aforementioned, the propeller model includes a twist section, which generates higher load (both lift and drag) values. Regarding drag force (Fig. 8(b)), the maximum drag occurs at approximately 60% of the propeller length. This corresponds to the region where both the twist and angle of attack of the propeller are at their highest. Beyond this point, the forces acting on the propeller surface decrease. A similar trend is observed for the lift force as well (see Fig. 8(a)).

In the conceptual design phase or sometimes before that, the efficiency of the propeller is needed for designers to calculate the maximum thrust value of an aircraft. This thrust value will be used to define endurance of an aircraft. In this regard, analytical methods suggested to identify the propeller efficiency (Glauert, 1935). Fig. 9 (a) indicates proposed propeller efficiency by changing advance ratio (J). It is worth mentioning that advance ratio depends on velocity, RPM and propeller's diameter. It can be seen that maximum propeller efficiency (η=0.79) achieved at J=0.51. Since efficiency is inversely proportional to the power coefficient, the propellers with higher power coefficient have lower efficiency. The data points show that as the Advance Ratio (J) increases, the efficiency of the propeller initially increases, reaches a peak, and then begins to decrease. At very low Advance Ratios (J = 0.10), the efficiency is very low. This is typical for situations where the propeller is spinning rapidly, but the forward speed is very low, such as during takeoff or when the air vehicle is stationary. As J increases (J = 0.51 to J = 0.64), the efficiency of the propeller peaks (J = 0.51). This range represents the optimal operating condition for the propeller, where it is most effective at converting engine power into thrust. At higher Advance Ratios (J > 0.64), the efficiency starts to decrease. This indicates that at higher speeds (relative to the propeller's rotational speed), the propeller becomes less efficient, likely due to aerodynamic losses and the reduced ability to generate thrust. For maximum fuel efficiency and performance, the aircraft should aim to operate at or near the Advance Ratio that corresponds to the peak efficiency. Consequently, the maximum efficiency occurs at a moderate Advance Ratio, suggesting that there is an optimal range of operating conditions where the propeller performs best. Low efficiency at very low and very high Advance Ratios indicates that the propeller is not well-suited for those conditions. At low J, the propeller is not effective because the forward speed is too low, and at high J, the propeller is less efficient because it cannot generate sufficient thrust relative to the power input. For maximum fuel efficiency and performance, the aircraft should aim to operate at or near the Advance Ratio that corresponds to the peak efficiency.

Moreover, Fig. 9 (b) illustrates the propeller thrust and power coefficient values versus advance ratio which play an important role in determining the power required to rotate the propeller. Taking as reference value of advance ratio (J=0.51) at which the propeller efficiency is highest, C_T and C_P values are found as 0.1 and 0.07, respectively. Looking details in graph, the x-axis represents the Advance Ratio (J), which is the ratio of the forward speed of the aircraft to the product of the propeller's rotational speed and diameter. The y-axis represents the values of the Thrust Coefficient (C_T) and the Power Coefficient (C_P). According to general trends, as the Advance Ratio (J) increases from 0.41 to 0.85, both C_T and C_P decrease. Thrust Coefficient (C_T) starts higher at lower advance ratios and decreases as the advance ratio increases. This indicates that the propeller is more effective at generating thrust at lower advance ratios (higher relative rotational speeds).

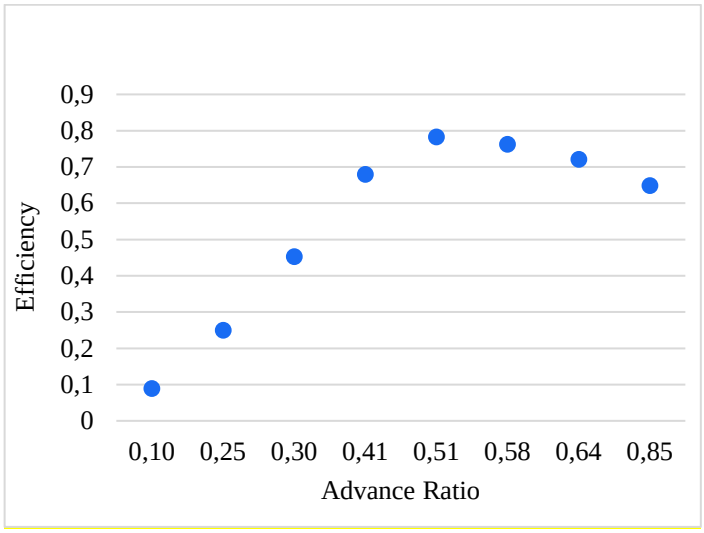

(a)

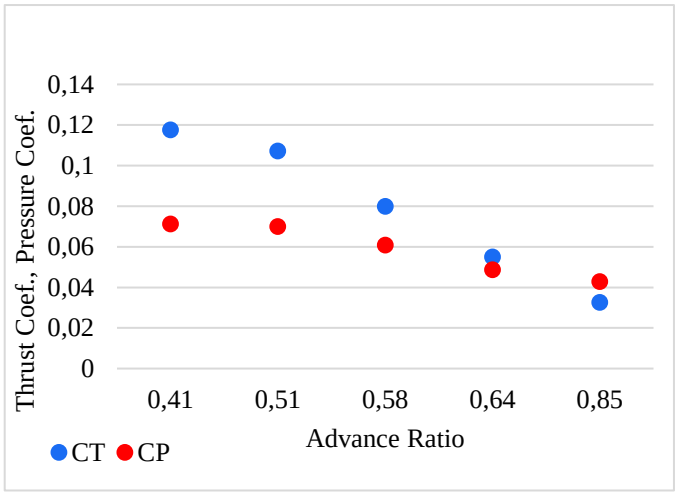

(b)

Fig. 9. Propeller performance values: (a) Propeller Efficiency and (b) Propeller Thrust Coefficient and Pressure Coefficient

Power Coefficient (C_P) also decreases with increasing advance ratio, but it does so more gradually compared to C_T. At lower Advance Ratios (e.g., J = 0.41): The propeller produces more thrust relative to power absorbed, indicated by higher C_T values. This is typical for takeoff or low-speed operations. At higher Advance Ratios (e.g., J = 0.85): Both C_T and C_P are lower, meaning that the propeller is operating in a more efficient regime, where less thrust and power are needed as the vehicle is moving faster. This is more representative of cruise conditions. The decreasing trend of both C_T and C_P with increasing J suggests that as the forward speed increases (relative to propeller speed), the propeller becomes less effective at generating thrust, and the power required to maintain that thrust also decreases. This graph is useful for understanding the performance of a propeller across different operating conditions, particularly how effective it is at converting rotational power into thrust at various speeds.

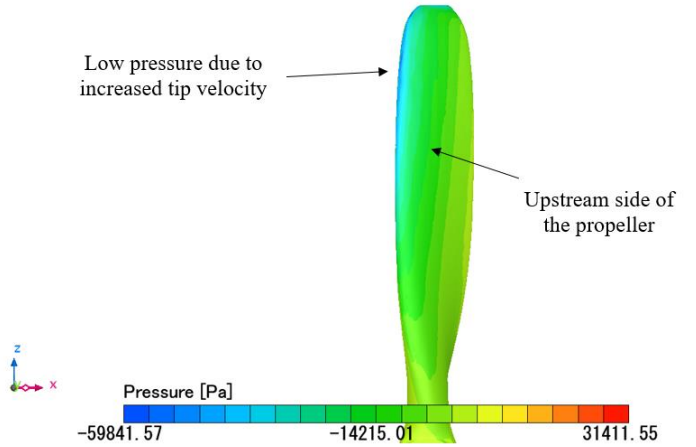

(a)

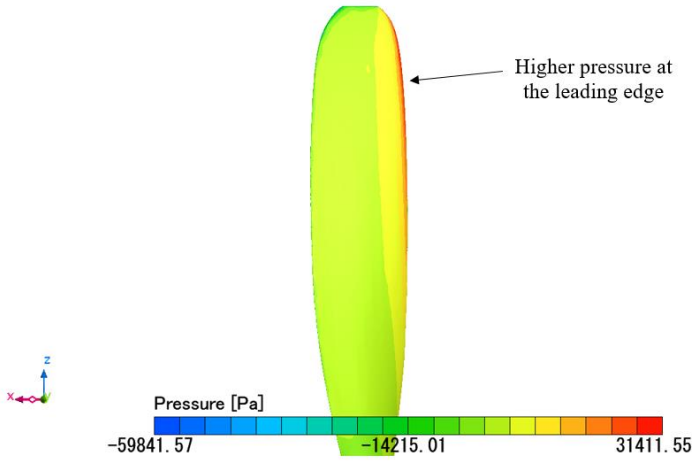

(b)

Fig. 10. Pressure distribution over the propeller: (a) pressure contours on the upstream side of the propeller (3100RPM) and (b) pressure contours on the downstream side of the propeller (3100RPM)

Fig. 10 (a) and (b) show the pressure contours on the propeller structure. With constant RPM (3100), the speed on the propeller sections increased proportionally from hub to tip. This causes a gradual decrease in pressure due to the increase in velocity from the hub to the tip as agreement with (Krishnan et al., 2009). Furthermore, the higher pressure is seen as expected at the front point where the propeller meets the fluid towards the direction of rotation. The downstream side of the propeller shows evenly distributed higher pressure; this flow creates a pressure difference with the unevenly distributed low pressure on the upstream and downstream sides, thus producing thrust.

4. Conclusions

Characterizing the aerodynamic performance of a propeller is essential for applications ranging from aviation to marine propulsion. It delivers insights that aid in the design process, ensuring that propellers perform

optimally under targeted operating conditions. In general, the fixed pitch produced propeller model has been analyzed aerodynamically in this research. As a result of this analysis, considering maximum 3100 RPM value;

- Propeller provided a thrust value of 1700N. This value was compared with the data obtained from experimental studies and the notable match was achieved.
- Aerodynamic performance data are considered; proposed propeller model was found to have 0.79 efficiency value at J=0.51.
- Thrust coefficient and pressure coefficient values are found as 0.1 and 0.07, respectively.
- When looking at the fluidity of the model, similar observation was achieved with theory.

As future work, the full range of efficiency of the propeller can be achieved by taking measurements at different RPM values, and the optimum angle of the propeller can be found by measurements made with different pitch angles.

Acknowledgment

This research is supported by Lentatek Aerospace, Aviation and Technology Inc. - R&D center, under 'Indigenous Propeller Project', No: AGTMPR90482.

CRediT Author Statement

Erdogan Kaygan: Conceptualization, Methodology, Software, Visualization, Investigation, Data curation, Writing- Original draft preparation. **Doğukan Doğan**: Methodology, Software, Data curation, Writing- Original draft preparation. **Ozan Mahir Alpagut**: Investigation, Supervision, Validation, Writing- Reviewing and Editing.

Nomenclature

C_L : Lift coefficient

C_D : Drag coefficient

C_T : Thrust coefficient

C_P : Power coefficient

η : Propeller efficiency

T : Thrust, N

ρ : Density, kg/m3

n : Rotational speed, rev/s

D : Diameter, m

J : Advance ratio

V : Freestream velocity, m/s

c : Chord length, m

r : Radial distance from hub centre, m

R : Propeller radius, m

μ_t : Turbulent viscosity

β : Pitch angle

References

Alakashi, A. M. and Basuno, I. B. (2014). Comparison between Structured and Unstructured Grid Generation on Two Dimensional Flows Based on Finite Volume Method (FVM), Int. J. Mining, Metall. Mech. Eng.

Asl, H. H., Monfared, A. R. K. and Manouchehr, R. (2017). Experimental investigation of blade number and design effects for a ducted wind turbine., Renewable Energy 105.

Bertetta, D., Brizzolara, S., Gaggero, S., Viviani, M., & Savio, L. (2012). CPP propeller cavitation and noise optimization at different pitches with panel code and validation by cavitation tunnel measurements. Ocean Engineering, 53, 177 195.

Brandt, J. and Selig, M. (2011). Small-Scale Propeller Performance at Low Speeds – Online Database, 49th AIAA Aerospace Sciences Meeting, Orlando, FL.

François G. Schmitt. (2007). About Boussinesq's turbulent viscosity hypothesis: historical remarks and a direct evaluation of its validity. Comptes Rendus Mécanique, 335 (9-10), pp.617-627. ff10.1016/j.crme.2007.08.004ff. ffhal-00264386

Glauert, H. (1935). "Airplane Propellers," Aerodynamic Theory: A General Review of Progress, edited by Durand, F. W., Vol. 4, Springer, Berlin.

Gur, O. (2013). Practical Propeller Efficiency Model, Proceedings of the 53rd Israel Annual Conference on Aerospace Sciences, Technion–Israel Institute of Technology Haifa, Israel.

Houghton and Carpenter., 2005. Aerodynamics for Engineering students, fourth edition.

Kaidi, S., Smaoui, H. and Sergent, P. (2012). CFD Investigation of Mutual Interaction between Hull, Propellers, and Rudders for an Inland Container Ship in Deep, Very Deep, Shallow, and Very Shallow Waters, J. Waterw. Port, Coastal, Ocean Eng., vol. 144, no. 6.

Kang, T., and Park., W.G. (2013). "Numerical investigation of active control for an S809 wind turbine airfoil," Int. J. Precis. Eng. Manuf., vol. 14, no. 6, pp. 1037–104.

Krishnan, P.S., Sathian, S. P. (2009). Numerical Investigation of VE-7 Airplane Propeller through CFD, Proceedings of ICEAE 2009.

Kutty, H. A., Parvathy, R. and Akshay, M. (2017). Performance analysis of small scale UAV propeller with slotted design. 2nd International Conference for Convergence in Technology (I2CT), pp. 695-700. IEEE. https://doi.org/10.1109/i2ct.2017.8226219

Lieser, J. A., Lohmann, D. and Rohardt, C. H. (1997). "Aeroacoustic design of a 6-bladed propeller." Aerospace science and technology1, no. 6: 381-389. https://doi.org/10.1016/s1270-9638(97)90012-2

Marcus, E. A. P., Vries, R. de, Kulkarni, A. Raju and Veldhuis, L. L. M. (2018). Aerodynamic Investigation of an Over-the-Wing Propeller for Distributed Propulsion, AIAA, Doi: 10.2514/6.2018-2053

McCormick, B. W. (1994). Aerodynamics, Aeronautics and Flight Mechanics, Johnwiley & sons Inc., second edition.

Ol, M., Zeune, C., and Logan, M. (2008). Analytical/Experimental Comparison for Small Electric Unmanned Air Vehicle Propellers, AIAA Paper 2008–7345,

Osborne, Reynolds (1895). On the Dynamical Theory of Incompressible Viscous Fluids and the Determination of the Criterion. Philosophical Transactions of the Royal Society of London A. 186: 123164. doi:10.1098/rsta.1895.0004. JSTOR 90643

Ramzi, M., Bois, G., Abderrahmane, G. and De Constantine, R. (2011). "Numerical Study of Passive Control with Slotted Blading in Highly Loaded Compressor Cascade at Low Mach Number," Int. J. Fluid Mach. Syst., vol. 4, no. 1, pp. 97–103.

Rezaeiha, A., Hamid M. and Bert B. (2019). On the accuracy of turbulence models for CFD simulations of vertical axis wind turbines. Energy180: 838-857. https://doi.org/10.1016/j.energy.2019.05.053

Sanjeevi, K., Sathish, P. & Sathian, Sarith. (2009). Numerical Investigation of VE-7 Airplane Propeller through CFD. IISc Centenary International Conference and Exhibition on Aerospace Engineering (ICEAE 2009), Bangalore, India

Seeni, A. (2019). Aerodynamic Performance Characterization of Slotted Propeller: Part B Effect of Angle. INCAS Bulletin11, no. 4: 155-170. https://doi.org/10.13111/2066-8201.2019.11.4.14

Seeni, A. and Rajendran, P. (2020). CFD Analysis of a Novel Propeller Design Operating at Low Reynolds Number. In: Rajendran, P., Mazlan, N., Rahman, A., Suhadis, N., Razak, N., Abidin, M. (eds) Proceedings of International Conference of Aerospace and Mechanical Engineering 2019, Springer, Singapore. https://doi.org/10.1007/978-981-15-4756-0_13

Seeni, A., Ismail, F., and Rajendran, P. (2020). The Aerodynamic Performance Characteristics of a Grooved Propeller Using a RANS solver: Effect of Groove Geometry and Positioning of Multiple Grooves. Proceedings of the International Conference on Innovations in Thermo-Fluid Engineering and Sciences [ICITFES - 2020] NIT Rourkela, India.

Singh, P. and Nestmann, F. (2011). "Experimental investigation of the influence of blade height and blade number on the performance of low head axial flow turbines." Renewable Energy36, no. 1: 272-281. https://doi.org/10.1016/j.renene.2010.06.033

Song X, Qi Y, Zhang M, Zhang G, Zhan W (2019) Application and optimization of drag reduction characteristics on the flow around a partial grooved cylinder by using the response surface method. Eng Appl Comput Fluid Mech 13(1):158–176

Tian, W., Song, B., Van Zwieten, J. H. and Pyakurel, P. (2015). Computational fluid dynamics prediction of a modified savonius wind turbine with novel blade shapes, Energies, vol. 8, no. 8, pp. 7915–7929.

Versteeg, H. and Malalasekera, W. (1995). An introduction to Computational Fluid Dynamics. Pearson Prentice Hall.

Wald, Q. R. (2006). The aerodynamics of propellers, Progress in Aerospace Sciences, Volume 42, Issue 2, 2006, Pages 85-128

Xie, Y., Chen, J., Qu, H., Xie, G., Zhang, D., and Moshfeghi, M. (2013). Numerical and Experimental Investigation on the Flow Separation Control of S809 Airfoil with Slot, Math. Probl. Eng., vol. 2013.

Zao, N., Dhanak, M., and Su, T. (2019). "Improved performance of a slotted blade using a novel slot design." Journal of Wind Engineering and Industrial Aerodynamics189: 34-44. https://doi.org/10.1016/j.proeng.2015.11.309